Adsorption (2011) 17:695–699
DOI 10.1007/s10450-011-9365-z

Solidification in weakly attractive cylindrical nanopores under tensile condition

Hideki Kanda

Received: 29 June 2010 / Accepted: 15 July 2011 / Published online: 2 August 2011

Abstract The authors clarified freezing points of the Lennard-Jones (LJ) condensate for strongly attractive cylindrical nanopores by using molecular dynamics (MD), and by thermodynamically predicting the results without using any adjustable parameters. In contrast to the Clapeyron equation, the obtained freezing points exhibited a significant dependence on the equilibrium bulk phase pressure, forming a remarkably skewed curve on a p–T diagram. In this paper, for weakly attractive cylindrical nanopores, freezing point depression under tensile conditions, similar to the authors previous study. The MD results show that the authors previous thermodynamic model successfully predicted freezing point depression for a bigger pore. However, for a smaller pore, obtained freezing points (liquid-solid coexistence curve) remarkably close to the bulk vapor-solid coexistence curve, and could not be predicted by the thermodynamic model.

Keywords Solidification · Thermodynamic model · Pore wall interaction · Molecular dynamics

1 Introduction

Freezing points depression in porous materials have been reported by several experimental studies (Patrik and Kemper 1938; Rennie and Clifford 1977; Tell and Maris 1983; Warnock et al. 1986; Torii et al. 1990; Sokol et al. 1992; Strange et al. 1993; Unruh et al. 1993; Moltz et al. 1993; Gelb et al. 1999). In contrast to these studies, it was clarified that the solidification mechanism in nanopores is more complex than textbook knowledge, the Gibbs-Thomson equation.

For slit pores, by using surface force apparatus, Klein and Kumacheva (Klein and Kumacheva 1995, 1998; Kumacheva and Klein 1998) found a freezing point elevation of cyclohexane and octamethylcyclotetrasiloxane confined between parallel mica plates. Theoretically, Miyahara and Gubbins (1997) clarified the origin of the freezing point elevation is pore wall potential. Later, many experiments including the authors (Kaneko et al. 1999; Watanabe et al. 1999; Sliwinska-Bartkowiak et al. 2001a, 2001b; Miyahara et al. 2002) have also reported freezing point elevations.

For cylindrical pores, freezing phenomena (Maddox and Gubbins 1997) and its physical modeling (Kanda et al. 2000) examined for Lennard-Jones (LJ) systems by molecular simulations. They found a nonmonotonic dependence of the freezing point on the pore diameter, which was induced by the geometric constraints and the potential effect of the pore wall. The geometric constraints originate from a solid-like (amorphous) phase in the cylindrical pore relative to the fcc lattice phase, which is known to increase in strength for smaller pore sizes. This geometric constraints depress the freezing point. But on the contrary, pore wall's potential is bigger in a smaller pore. This effect raise the level of the freezing point. These two conflicting effects are cause of the nonmonotonic dependence of the freezing point on the pore diameter (Kanda et al. 2000).

In addition the authors (Miyahara et al. 2000; Kanda et al. 2004; Kanda and Miyahara 2007) found the freezing point depression of capillary-condensate in nanopores below the saturation pressure by molecular dynamics simulations. The obtained freezing points exhibited a significant dependence on the equilibrium bulk-phase pressure, forming a remarkably skewed curve on a pressure-temperature

H. Kanda (✉)
Energy Engineering Research Laboratory, Central Research Institute of Electric Power Industry, Yokosuka, Kanagawa 240-0196, Japan
e-mail: kanda@criepi.denken.or.jp

(p–T) diagram, in contrast to the bulk-phase coexistence that had an almost vertical line (Clapeyron equation). This was attributed to the tensile (Laplace) effect. The inner pressure of the capillary condensate is lowered to a negative value by the strong tensile effect. The authors present a simple model in which the Clapeyron equation is applied to the inner pressure. The freezing point depression is thermodynamically modeled.

However, these studies were mainly concerned with the freezing phenomena in strongly attractive nanopores. In other words, the freezing point elevation by the potential effect is superior to the freezing point depression by the geometric constraints. This conditions were contradictory to freezing depression observed in usual experiments. In this study, the freezing point depression of LJ methane under tensile conditions in a weakly attractive cylindrical pore is examined.

2 MD simulation method

We employed the MD technique with the boundaries of the vapour phase to obtain the variations in the bulk vapour pressure. The unit cell and technique were same as that employed in the previous study (Kanda and Miyahara 2007). NVT-MD technique with vapor phases (Kanda et al. 2004) was employed to obtain the bulk vapor pressure as the result of the simulation. As shown in Fig. 1, the middle of the unit cell is the pore space with a given pore wall interaction. Between the vapor phases and the edges of the pore space, slopes of the pore wall interaction were set, since the pore wall interaction must be zero in the vapor phases. The bulk vapor pressure was directly obtained by collision frequency of fluid particles at the border plane of the vapor phases. A simulation run for a given number of fluid particles was started with an initial configuration arranged in the form of a liquid-like phase. Initially, the temperature of the system was controlled by velocity scaling once every 100 steps for 1000 ps. Each run lasted at least 50,000 ps with a time increment of 5 fs; the duration of each run was determined such that the number of particles reaching the border plane was 500 or more. The final configuration, obtained at a higher temperature, was used for the initial configuration at a lower temperature. Methane fluid was modeled using a truncated and shifted LJ (12-6) potential: $\varepsilon_{\mathrm{ff}}/k = 148.1$ K and $\sigma_{\mathrm{ff}} = 0.381$ nm. The cut-off distance of the adsorbate was $5\sigma_{\mathrm{ff}}$.

For the pore potential, a cylindrical pore surrounded by a semi-infinite solid was used with cylindrical coordinate integration (Peterson et al. 1986). At a radial position r, where $r = 0$ at center of pore, the interaction between a fluid particle and the pore wall with radius R is given as:

$$\phi_{\mathrm{fs}}(r, R) = \pi \varepsilon_{\mathrm{fs}} \chi \rho_{\mathrm{s}} \left(\frac{7\sigma_{\mathrm{fs}}^{12}}{32} K_9(r, R) - \sigma_{\mathrm{fs}}^{6} K_3(r, R) \right) \quad (1)$$

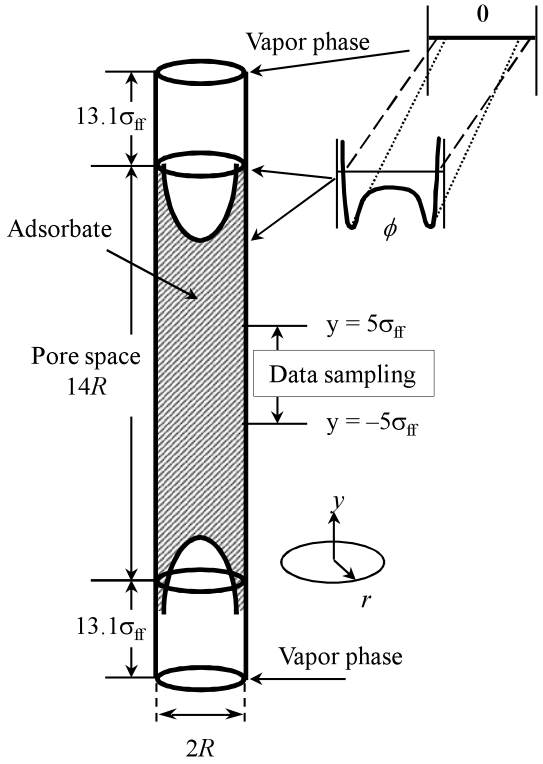

Fig. 1 Unit cell with bulk vapor phase

where

$$K_{\mathrm{n}}(r, R) = R^{-n} \int_0^{\pi} \mathrm{d}\Theta \left(-\frac{r}{R} \cos\Theta + \left(1 - \left(\frac{r}{R} \right)^2 \sin^2\Theta \right)^{1/2} \right)^{-n},$$

r is the distance between a fluid particle and the center of the surface atoms of the wall, and the parameters $\varepsilon_{\mathrm{ss}}/k$ and σ_{ss} are set to 28.0 K and 0.340 nm, respectively. Other constants are assumed as follows: the mass of methane, m was set to 2.665×10^{-26} kg and the pore diameters D were $5.5\sigma_{\mathrm{ff}}$, $7.5\sigma_{\mathrm{ff}}$, and $9.5\sigma_{\mathrm{ff}}$. ρ_{s} is the normal number density of the interaction sites in the carbon wall, and has a value of 1.14×10^{29} m^{-3}. χ is an interaction parameter having values of 0.80, 0.65, and 0.75 for $D = 5.5\sigma_{\mathrm{ff}}$, $7.5\sigma_{\mathrm{ff}}$, and $9.5\sigma_{\mathrm{ff}}$, respectively. The above settings of χ were used to obtain the same freezing point, 98 K, at the bulk saturation vapor pressure for each pore diameter. In this condition, since the geometrical hindrance effect is stronger than pore wall's potential effect, freezing point is lower than the bulk freezing point 101 K (Kanda et al. 2000).

A simulation was performed for a given number of fluid particles N starting from an initial configuration of an arrangement as a liquid-like phase. The temperature of the system was controlled by velocity scaling once every 100 steps during the initial 1000 ps. The leapfrog Verlet method was used to numerically integrate the equations of motion. Each

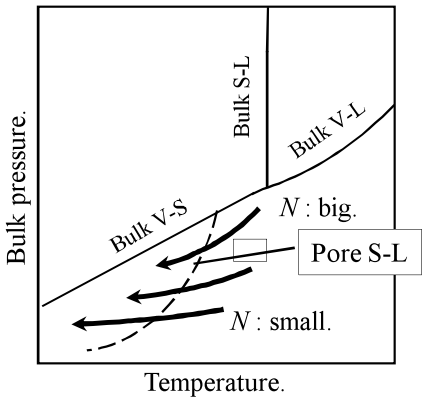

Fig. 2 Scheme of the operating p–T conditions in the simulations

run lasted at least 50000 ps with a time increment of 5 fs; this duration was used so that the number of particles reaching the border plane was approximately 500 or more. The total number of particles in the cell, N, ranged from 700 to 900 for $D = 5.5\sigma_{\mathrm{ff}}$, 1200 to 1750 for $D = 7.5\sigma_{\mathrm{ff}}$, and 2800 to 3700 for $D = 9.5\sigma_{\mathrm{ff}}$, depending on the expected pressure condition. The final configuration obtained at a higher temperature was used as the initial configuration at a lower temperature. The operating p–T conditions in this sequence are indicated by the bold curves in Fig. 2. The value of the equilibrium bulk pressure is higher at higher values of N.

3 Results and discussion

The typical results for variation in the overall density on cooling from a higher temperature are shown in Fig. 3. The overall density, ρ^*, of the adsorbate in the pore is expressed as follows:

$$\rho^* = \rho\sigma_{\mathrm{ff}}^3 : \rho = \frac{\langle N\rangle}{V} \qquad \text{and} \qquad V = \frac{D^2}{4}\pi \times 10\sigma_{\mathrm{ff}}, \quad (2)$$

where $\langle N\rangle$ denotes the ensemble average of the number of fluid particles between $-5\sigma_{\mathrm{ff}} < y < 5\sigma_{\mathrm{ff}}$. V is taken as the volume of the space. At higher temperatures, the density exhibits a gradual increase, indicating a liquid-like structure, as shown by open circles in Fig. 3. The density exhibits an almost vertical change around the freezing points with little cooling, while in the lower temperature range, a slight variation in the density is recognizable as shown by closed circles in Fig. 3. Starting from the last configuration of the run at the lowest temperature, heating series of simulations were also carried out to examine the hysteresis between cooling and heating. The results are superimposed in Fig. 3. Open triangles and closed triangles indicate respectively liquid-like structure and solid-like structure in the heating. Small amounts of hysteresis was found for each pore size. However, there seems to exist no definitive relationship between

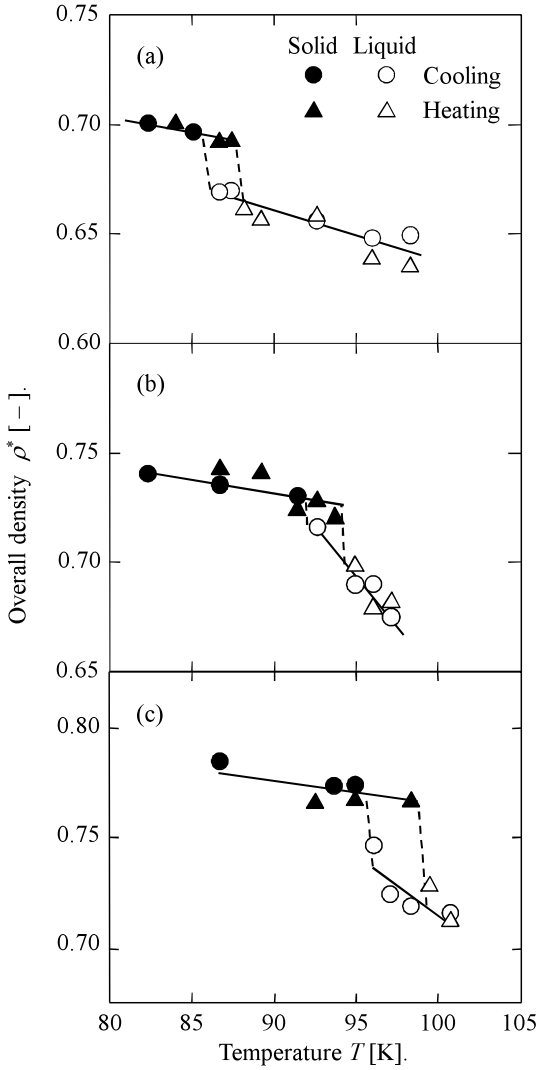

Fig. 3 Density profile within the pore. (**a**) $D = 5.5\sigma_{\mathrm{ff}}$, $N = 775$, $\chi = 0.80$; (**b**) $D = 7.5\sigma_{\mathrm{ff}}$, $N = 1650$, $\chi = 0.65$; and (**c**) $D = 9.5\sigma_{\mathrm{ff}}$, $N = 3600$, $\chi = 0.75$

the extent of the hysteresis and the pore width. As reported earlier (Miyahara and Gubbins 1997), the freezing branch was considered to be closer to the true transition point than the melting branch. Here in this study, freezing points in the cooling branch were mainly discussed. Under these conditions, liquid-solid phase transition were not detected clearly by in-plane pair distribution function in cylindrical coordinate. Then, in this study, transition is examined with the overall density.

The above set of simulations was performed for various values of N and the coexistence points were determined as shown in Fig. 4. Open circles represent the liquid-like phase and closed triangles represent the solid-like phase. The thin curves represent the bulk phase sublimation curves. Bold solid lines represent the predictions made by the authors' simple model (Kanda and Miyahara 2007) with the bulk

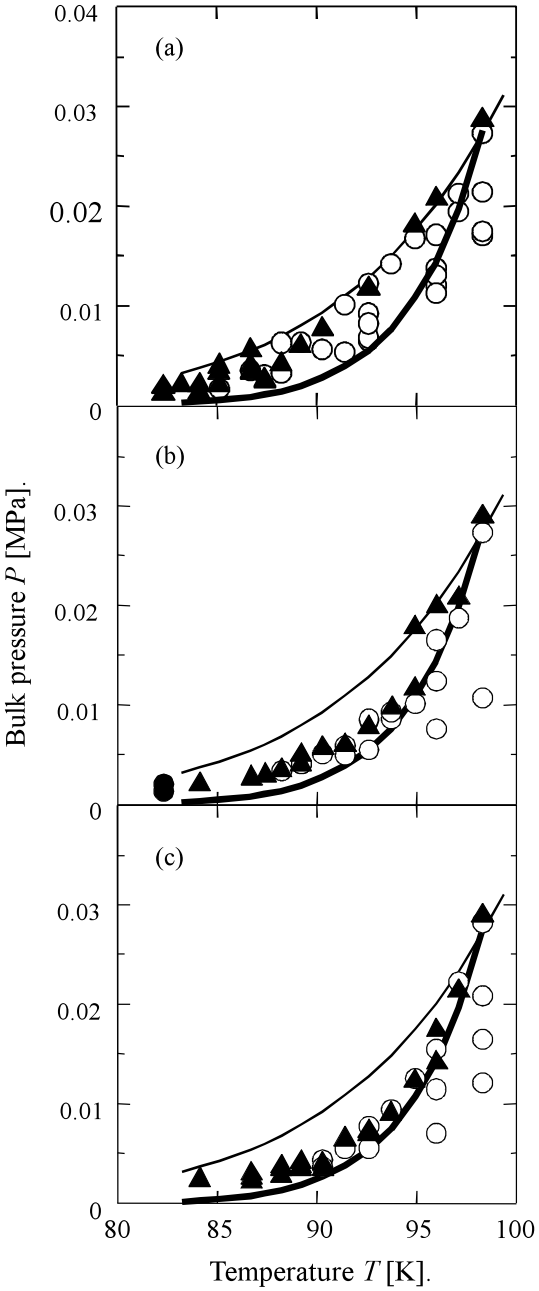

Fig. 4 Phase condition within the pore for various pore diameters obtained from the MD simulations (keys), superimposed on the bulk phase diagram (*thin solid lines*). (**a**) $D = 5.5\sigma_{\mathrm{ff}}$; (**b**) $D = 7.5\sigma_{\mathrm{ff}}$; and (**c**) $D = 9.5\sigma_{\mathrm{ff}}$

solid's properties (Agrawal and Kofke 1995). Normal bulk fluids exhibit only a weak change in the freezing point with pressure. The salient feature of this figure is the remarkable dependence of the freezing point on the bulk-phase pressure below the saturated vapor pressure of the bulk phase. The overlapping portions of the open triangles and closed circles show the solid-liquid coexistence points obtained by the MD simulation. For $D = 9.5\sigma_{\mathrm{ff}}$, the solidification points are successfully predicted by the authors' simple model. However, for smaller pores, the disagreement between the MD results and the prediction of the model becomes larger. In particular, for $D = 5.5\sigma_{\mathrm{ff}}$, the MD results implied that the solidification points almost overlap the bulk sublimation line. This phenomenon was not observed for a strongly attractive pore (Kanda and Miyahara 2007). The result indicates that if freezing point depression is observed at the saturation pressure for smaller pore, a significant error in the prediction by using the authors model. This information is important for the ongoing experimental studies.

4 Conclusion

The effect of the equilibrium vapor-phase pressure on freezing in a cylindrical pore was examined by employing the MD technique using an imaginary vapor phase. The MD simulations revealed liquid-solid phase transitions with a variation in the equilibrium vapor-phase pressure below the saturated pressure. Therefore, the computed solid-liquid coexistence line exhibited a significant dependence of the freezing point against a small change in the bulk-phase vapor pressure, which suggests the importance of the tensile effect on freezing in nanopores. In addition, the solid-liquid coexistence curve of the pore fluid is remarkably close to the bulk vapor-solid coexistence curve. This observation implies that in a real examination, the vapor pressure around a porous material is very important since a slight depression in the pressure below the saturated bulk pressure causes a significant error in the melting point. In particular, the solid-liquid coexistence curve is remarkably close to its solid-vapor bulk curve for micropores.

References

Agrawal, R., Kofke, D.A.: Mol. Phys. **85**, 43–59 (1995)
Gelb, L.D., Gubbins, K.E., Radhakrishnan, R., Sliwinska-Bartkowiak, M.: Rep. Prog. Phys. **62**, 1573–1659 (1999)
Kanda, H., Miyahara, M.: Adsorption **13**, 191–195 (2007)
Kanda, H., Miyahara, M., Higashitani, K.: Langmuir **16**, 8529–8535 (2000)
Kanda, H., Miyahara, M., Higashitani, K.: J. Chem. Phys. **120**, 6173–6179 (2004)
Kaneko, K., Watanabe, A., Iiyama, T., Radhakrishnan, R., Gubbins, K.E.: J. Phys. Chem. B **103**, 7061–7063 (1999)
Klein, J., Kumacheva, E.: Science **269**, 816–819 (1995)
Klein, J., Kumacheva, E.: J. Chem. Phys. **108**, 6996–7009 (1998)
Kumacheva, E., Klein, J.: J. Chem. Phys. **108**, 7010–7022 (1998)
Maddox, M.W., Gubbins, K.E.: J. Chem. Phys. **107**, 9659–9667 (1997)
Miyahara, M., Gubbins, K.E.: J. Chem. Phys. **106**, 2865–2880 (1997)
Miyahara, M., Kanda, H., Shibao, M., Higashitani, K.: J. Chem. Phys. **112**, 9909–9916 (2000)
Miyahara, M., Sakamoto, M., Kanda, H., Higashitani, K.: Stud. Surf. Sci. Catal. **144**, 411–418 (2002)
Moltz, E., Wong, A.P.Y., Chan, M.H., Beamish, J.R.: Phys. Rev. B **48**, 5741–5750 (1993)
Patrik, W.A., Kemper, W.A.: J. Phys. Chem. **42**, 369–380 (1938)

Peterson, B.K., Walton, J.P.R.B., Gubbins, K.E.: J. Chem. Soc. Faraday Trans. II **82**, 1789–1800 (1986)

Rennie, G.K., Clifford, J.: J. Chem. Soc. Faraday Trans. I **73**, 680–689 (1977)

Sliwinska-Bartkowiak, M., Dudziak, G., Sikorski, R., Gras, R., Gubbins, K.E., Radhakrishnan, R.: Phys. Chem. Chem. Phys. **3**, 1179–1184 (2001a)

Sliwinska-Bartkowiak, M., Radhakrishnan, R., Gubbins, K.E.: Mol. Simul. **27**, 323–337 (2001b)

Sokol, P.E., Ma, W.J., Herwig, K.W., Snow, W.M., Wang, Y., Koplik, J., Banavar, J.R.: Appl. Phys. Lett. **61**, 777–779 (1992)

Strange, J.H., Rahman, M., Smith, E.G.: Phys. Rev. Lett. **71**, 3589–3591 (1993)

Tell, J.L., Maris, H.J.: Phys. Rev. B **28**, 5122–5125 (1983)

Torii, R.H., Maris, H.J., Seidel, G.M.: Phys. Rev. B **41**, 7167–7181 (1990)

Unruh, K.M., Huber, T.E., Huber, C.A.: Phys. Rev. B **48**, 9021–9027 (1993)

Warnock, J., Awschalom, D.D., Shafer, M.W.: Phys. Rev. Lett. **57**, 1753–1756 (1986)

Watanabe, A., Iiyama, T., Kaneko, K.: Chem. Phys. Lett. **305**, 71–74 (1999)